Title

The ICCAM platform study: An experimental medicine platform for evaluating new drugs for relapse prevention in addiction. Part B: fMRI description

Running head

ICCAM platform: fMRI description

Keywords

Brain

Human

Magnetic Resonance Imaging

Substance-Related Disorders

Authors

John McGonigle[1]

Anna Murphy[2]

Louise M Paterson[1]

Laurence J Reed[1]

Liam Nestor[1,4]

Jonathan Nash[1]

Rebecca Elliott[2]

Karen D Ersche[3,4]

Remy SA Flechais[1]

Rexford Newbould[5]

Csaba Orban[1]

Dana G Smith[3]

Eleanor M Taylor[2]

Adam D Waldman[6]

Trevor W Robbins[3,7]

JF William Deakin[2]

David J Nutt[1]

Anne R Lingford-Hughes[1]

John Suckling[3,4,8]

ICCAM Platform[*]

Affiliations

1. Centre for Neuropsychopharmacology, Division of Brain Sciences, Imperial College London, UK

2. Neuroscience and Psychiatry Unit, Institute of Brain, Behaviour and Mental Health, The University of Manchester, UK

3. Behavioural and Clinical Neuroscience Institute, University of Cambridge, UK

4. Department of Psychiatry, University of Cambridge, UK

5. Imanova Limited, London, UK

6. Centre for Neuroinflammation and Neurodegeneration, Division of Brain Sciences, Imperial College London, UK

7. Department of Psychology, University of Cambridge, UK

8. Cambridgeshire and Peterborough NHS Foundation Trust, UK

[*]ICCAM Platform collaborators are named in the Acknowledgements section

Address for correspondence

Anne Lingford-Hughes, Centre for Neuropsychopharmacology, Imperial College London, Burlington Danes Building, Hammersmith Hospital campus, 160 Du Cane Road, London, W12 0NN, UK.

Abstract

Objectives

We aimed to set up a robust multi-centre clinical fMRI and neuropsychological platform to investigate the neuropharmacology of brain processes relevant to addiction – reward, impulsivity, and emotional reactivity. Here we provide an overview of the fMRI battery, carried out across three centres, characterising neuronal response to the tasks, along with exploring inter-centre differences in healthy participants.

Experimental Design

Three fMRI tasks were used: monetary incentive delay to probe reward sensitivity; go/no-go to probe impulsivity; and an evocative images task to probe emotional reactivity. A coordinate-based activation likelihood estimation (ALE) meta-analysis was carried out for the reward and impulsivity tasks to help establish region of interest (ROI) placement. A group of healthy participants was recruited from across three centres (total n=43) to investigate inter-centre differences.

Principle Observations

The pattern of response observed for each of the three tasks was consistent with previous studies using similar paradigms. At the whole brain level, significant differences were not observed between centres for any task.

Conclusions

In developing this platform we successfully integrated neuroimaging data from three centres, adapted validated tasks, and applied whole brain and ROI approaches to explore and demonstrate their consistency across centres.

Introduction

Addiction is a major global health problem with illicit drug and alcohol use disorders contributing to approximately 20% of the burden from mental health disorders (Whiteford et al., 2013). Of concern is the lack of effective interventions for these disorders whilst the prevalence of alcohol, opioid and cocaine addiction is increasing (Lingford-Hughes et al., 2012; Whiteford et al., 2013). The growing knowledge about the brain mechanisms underpinning addiction offers an important opportunity to develop new treatments. Studying the neurobiology of addiction can be challenging due to its common relapsing remitting clinical course. To address this, a collaboration between Imperial College London, the University of Cambridge and The University of Manchester (ICCAM; http://www.bbmh.manchester.ac.uk/ICCAM/) was formed under a Medical Research Council (MRC) addiction initiative to maximise the existing MRI and clinical infrastructure and expertise available in the UK. Establishment of a platform is necessary to provide sufficient throughput to rapidly evaluate potential pharmacological treatments in addiction to allow us the best chance of meeting this area of significant unmet need. Here, the term 'platform' refers to the concept of applying a framework of experimentation (i.e. the fMRI tasks and associated measures) and analysis that can be applied under different conditions and on different groups to

accelerate efforts to identify effective treatments for challenging diseases (Berry et al., 2015).

The rationale for the cognitive processes and neuropharmacology as well as clinical population studied in the ICCAM platform have been described in detail elsewhere (Paterson et al., 2015). Its aim was to develop a neuroimaging platform to assess candidate brain pathways underpinning addiction and relapse using appropriate fMRI tasks and assessing their modulation by different pharmacological challenges (antagonists of Dopamine Receptor D3 (DRD3), μ-opioid receptors, and Neurokinin 1 (NK1) receptors). We were also interested in exploring whether any dysregulation was specific to addiction per se or to a particular substance. Therefore we recruited alcohol, heroin, and cocaine addicts to compare with healthy non-addicted controls. Results from these investigations will be reported elsewhere – this paper focuses on describing the establishment of fMRI tasks in the three centres in healthy volunteers and investigating their properties, however, we briefly describe our choice of cognitive processes and tasks.

fMRI tasks

In addiction, common themes implicated in relapse involve difficulties with reward or motivation, impulse control, as well as stress-related emotional reactivity. There is a considerable body of evidence from neuroimaging studies that a dysregulated reward/motivation system in addiction as well deficits in inhibitory control and poor decision making (Loree et al., 2014; Noel et al., 2013), and stress (Koob and Kreek, 2007; Sinha and Li, 2007) contribute to relapse. We therefore selected established fMRI tasks designed to elucidate the neural responses associated with these processes – reward/motivation, impulse control and emotional reactivity.

For reward, we chose the widely used monetary incentive delay task since it provides a measure of reward sensitivity with robust increases in striatal activity evident in healthy volunteers (Knutson et al., 2001). Striatal activity has been shown to be reduced in alcohol dependence (Wrase et al., 2007), and in stimulant use related to treatment status (Bustamante et al., 2014; Jia et al., 2011; Schouw et al., 2013). Furthermore, ventral striatal activation in response to the task is sensitive to pharmacological modulation by amphetamines (Knutson et al., 2004), olanzapine (Schlagenhauf et al., 2008), and catecholamine depletion (Hasler et al., 2009).

For impulsivity, we chose the go/no-go task since it provides a measure of inhibitory control mediated by prefrontal-striatal circuits (Garavan et al., 2002; Garavan et al.,

2003: 2003). Neural responses during go/no-go have been shown to be altered in cocaine users (Connolly et al., 2012; Kaufman et al., 2003), opiate addiction (Forman et al., 2004), and to be modulated by certain dopaminergic gene variants in heavy drinkers (Filbey et al., 2012).

To explore stress we exploited the associated emotional dysregulation since amygdalar response is robustly observed and altered in a range of neuroimaging studies of addicts (Li and Sinha, 2008; Asensio et al., 2010; Gilman and Hommer, 2008). Therefore, in common with others, we used an evocative images task to assess emotional reactivity to contrasting aversive images with neutral images from the International Affective Picture System (IAPS) library. Photographs containing scenes of animate and inanimate objects or scenes were displayed in a block-design, with each block containing either neutral or distressing images of an injurious or threatening nature. In addition due to studying addiction to different substances and therefore potentially variable cue-reactivity, images had no explicit alcohol/drug content. Similar tasks have been shown to elicit amygdala responses and have been employed to demonstrate enhanced responses in alcohol dependence (Gilman and Hommer, 2008: 2008) that were decreased by an NK1 receptor antagonist (George et al., 2008).

Meta-Analyses

Regions of interest (ROIs) are often used to examine response at one location or small region in the brain, as opposed, or in addition to, a more exploratory whole brain analysis. These are often chosen based on an investigator's knowledge of where a task has been found to modulate activity in previous work. A more formal way of establishing an appropriate a priori ROI is to carry out a coordinate-based meta-analysis of neuroimaging data using activation likelihood estimation (ALE) (Turkeltaub et al., 2002), and its later developments (Eickhoff et al., 2009; Turkeltaub et al., 2012; Eickhoff et al., 2012).

Several studies have used these methods to establish locations of consistent response to reward (Bartra et al., 2013; Keuken et al., 2014), impulsivity (Simmonds et al., 2008; Criaud and Boulinguez, 2013), and emotional reactivity (Fusar-Poli et al., 2009). However, there is much variation in the specifics of fMRI tasks, even amongst those considered as 'standard', with meta-analyses often using relatively broad inclusion criteria. These have the advantage of increased statistical power at the expense of reduced specificity. Here we seek to establish not only the general neural correlates of the paradigms under investigation, but also those elicited by the specific forms of each task as they were implemented.

Multi-Centre Studies

The advantages of multi-centre study designs are numerous and well-rehearsed (Paterson et al., 2015). Their increased throughput is especially important in a platform study where the aim is to quickly establish if a treatment is effective so that decisions may be made on what investigations are to be carried out in the next iteration of the research program. Furthermore, the heterogeneous aetiology and clinical presentations of many disorders make extensive and widespread sampling of an affected population essential for proper characterisation.

The involvement of multiple acquisition centres introduces new factors that require appropriate consideration during subsequent analysis. In particular, the overall variance is inflated by a between-centre factor and the potential for bias should a sub-set of centres have significantly greater statistical power than the others.

In this paper we detail both the specific forms of the tasks used in the platform study, along with their modelling, sufficient to enable replication. Following this, and taking each task in turn, we establish their characteristics before investigating inter-centre differences.

Methods

The study was conducted in accordance with the Declaration of Helsinki. Ethical approval was obtained from West London & GTAC NRES committee and relevant Research Governance and PIC (Participant Identification Centre) approvals obtained. Data were collected at three UK centres: Imanova Limited, London; The Wolfson Brain Imaging Centre, University of Cambridge; Salford Royal NHS Foundation Trust, Manchester.

Participants

Out of the 155 participants who had a full baseline imaging session in the main ICCAM study, 68 were healthy controls with no history of drug or alcohol dependence (19, 33, and 16 from London, Cambridge, and Manchester respectively) – only this group is examined further here. These were recruited from healthy volunteer databases, via multimedia advertising including fliers, posters, social media, local newspapers, websites, homepage, and via word of mouth.

From this group of 68 a subgroup of 43 (n = 15, 15, and 13 from London, Cambridge, and Manchester respectively) were chosen so that each centre had a similar distribution

of gender and age. This group of 43 healthy individuals was used for both the task characterisation and inter-centre variability investigations.

fMRI Task Protocols

E-Prime 2.0 RC (version 2.0.8.90) was used to run all tasks. Tasks were adapted such that two runs of each (along with resting state and preliminaries) could be achieved within a one hour period.

Monetary Incentive Delay Task

The Monetary Incentive Delay task, designed to probe the reward sensitivity, was modified from Knutson et al. (2001). Participants could win or lose money depending upon how quickly they reacted to a target stimulus. The task contained win, loss and neutral trials. For the win trials, participants could win £0.50 if they responded quickly enough; for the loss trials, participants lost £0.50 if they did not respond quickly enough; and for the neutral trials participants neither won nor lost money. During each run, 216 volumes were collected, for a run length of 7 min 12 s.

This task used an event related design, though with long mini-blocks, carried out in 2 runs. Each run contained 18 win trials, 18 neutral trials, and 6 loss trials. In total, the task contained 36 win trials, 36 neutral trials and 12 loss trials. The task was set to obtain approximately 66% accuracy for the win trials. Furthermore, the task was designed to give an approximate winnings total of £10 (a perfect, though unlikely, result would result in winnings of £18).

Participants were informed as to what trial they were about to perform via 'cues' that appeared on the screen for one second. Following the cues, there was an anticipation period (i.e. a black screen) before the target stimulus was presented. The duration of the anticipation period was randomly selected as 2, 3 or 4 s (with equal numbers of each period for each trial type). The anticipation period was immediately followed by the presentation of the target stimulus. The duration of the target stimulus differed depending upon the accuracy of participants.

The starting duration for the win and neutral trials was 280 milliseconds (ms) for both runs (i.e. the time allowed for a participant to press the button after the stimulus was displayed). For the individualised algorithm, if a participant responded in time for the target stimulus, the target duration dropped by 10 ms (until the floor duration of 150 ms was reached). If the participants missed a trial, the target duration increased by 10 ms

(until the ceiling duration of 300 ms was reached). The duration of each of the target symbols for each trial (win, neutral, loss) was contingent upon the participant's accuracy for the same trial type only, i.e. win trial accuracy only affected stimulus duration of subsequent win trials, and not neutral or loss trials. Participants were informed if they were successful after each trial, together with a display of their total winnings, which was shown for 2 s. For each trial type the interval between the end of this information/winnings display, and the onset of the next cue were 2.4, 3.4, or 4.4 s, with equal numbers of each period across trial types.

The starting duration for the loss trials was 240 ms for both runs. A reduced loss starting duration was chosen as we required participants to lose in order to increase the incentive salience of reward trials. A fixation cross was displayed for 12 s at the beginning of each run.

Go/No-Go Task

The Go/no-go task, designed to probe impulsivity, was modified from Garavan et al. (2002). Participants were presented with an alternating series of letter Xs and letter Ys and asked to respond as fast as they could to the appearance of each letter presented ('go' trial), except when the alternating sequence was broken by the appearance of a

letter the same as that presented previously ('no-go' trial). During each run, 131 volumes were collected, for a run length of 4 min 22 s.

This task used an event related design and was carried out in 2 runs. Each run contained 250 trials. 220 of these were 'go' trials where participants had to respond, and 30 of these trials were 'no-go' trials where the participant had to withhold a response (i.e. when the letter was the same as the previous letter). On average there was one 'no-go' trial every 8 s (range: 4 – 14 s).

Each letter was presented on the screen for 900 ms and was followed by a 100 ms inter-stimulus interval consisting of a blank screen. A fixation cross was displayed for 12 s at the beginning of each run.

Evocative Images Task

The Evocative Images task was designed to probe emotional reactivity. Participants were presented with aversive IAPS images containing scenes of injury or threat and neutral IAPS images containing scenes of animate and inanimate objects. Participants had to press their response pad to each image to ensure they were awake and attending

to the images. During each run, 196 volumes were collected, for a run length of 6 min 32 s.

The task used a block design and was carried out in 2 runs. Each run contained 4 blocks of aversive images and 4 blocks of neutral images. Each block contained 6 images and each block was separated by a rest period to prevent carry-over effects. Images in each block were presented in a pseudorandomised order. The second run of the task contained the same images as the first run, but presented in a different order. Due to possible habituation effects, different images were presented at each session.

Each block was 32.4 s (6 images of 5 s duration followed by a 400 ms inter-stimulus interval). Each rest period lasted 15 s. A fixation cross was displayed for 12 s at the beginning of each run.

ALE Meta-Analyses

To identify appropriate regions of interest (ROIs) for specific analyses, Activation Likelihood Estimation (ALE) meta-analyses (Eickhoff et al., 2009) of the literature were carried out using the BrainMap Project's GingerALE version (2.3.1) for both the monetary incentive delay and go/no-go tasks.

The following general study selection criteria were applied: (i) participants' mean age greater than 25 years (to preclude those studies focusing on young adults or children); (ii) used only one form of response (i.e. a single button for input); (iii) reported activation foci in either Talairach or MNI space; (iv) published in English; (v) appeared in a peer reviewed publication; (vi) used human participants; (vii) used greater than 6 participants; (viii) published between January 2002 and April 2013. Only healthy control data used if a study included other groups.

Monetary incentive delay studies were identified by searching the PubMed database using the terms: ('monetary' OR 'money' OR 'anticipation') AND ('fMRI' OR 'neuroimaging'); and by searching the BrainMap database (Fox et al., 2005) using the filters 'fMRI' and 'reward'. In order to identify previous studies with comparable versions of the monetary incentive delay task examined here, these further criteria were used: (i) participants actually paid their winnings; (ii) loss trials present; (iii) more than 10 gain trials; (iv) reward anticipation modelled against neutral anticipation.

Go/no-go studies were identified by searching the PubMed database using the terms: ('go/no-go' OR 'response inhibition') AND ('fMRI' or 'neuroimaging'); and by searching the BrainMap database using the filters 'fMRI' and 'go/no-go'. In order to

identify previous studies with comparable versions of the go/no-go task examined here, these further criteria were used: (i) no-go trials make up fewer than 40% of all trials; (ii) not include an oddball stimuli; (iii) use only letters (not images); (iv) use only 1 no-go cue; (v) correct no-go modelled against either correct go or an implicit baseline.

For studies that reanalysed previously used data, only the original studies were used. All coordinates were transformed into MNI space as necessary. ALE was performed for each task with a False discovery rate (FDR) of $p < 0.05$ (corrected) and a minimum cluster volume of 600 mm^3 (0.6 ml).

For each task, an ROI was made up of two 5 mm radius spheres placed bilaterally such that they overlapped with the weighted centre coordinates of the strongest bilateral ALE clusters while robustly covering grey matter.

Defining Regions of Interest: Evocative Images Task

Although emotional imaging tasks have been used in many previous studies, the considerably variability in the design (especially in the specific images used within) precludes a meta-analysis using the criteria used for the other tasks here. We therefore selected the bilateral amygdala as a key region of interest, based on the previous

literature with a range of emotional tasks (Phan et al., 2002). Thus, the ROI for the evocative images task was made up of two 5 mm radius spheres centred at the MNI coordinates [±22, -4, -12 mm] so as to be robustly in the grey matter of the amygdala as defined functionally by the clusters reported in a previously published ALE meta-analysis of amygdala responsivity (Costafreda et al., 2008).

MRI Data Acquisition

All centres operated MRI machines with a main magnetic field of 3 tesla (T). Centres in London and Cambridge operated nominally identical 3T Siemens Tim Trio systems running the syngo MR B17 software with a Siemens 32 channel receive-only phased-array head coil. The Manchester centre operated a 3T Philips Achieva running version 2.6.3.5 software and an 8 element SENSE head coil.

At each visit the imaging session consisted of: localiser scans to set up the positioning of those that would follow; main magnetic field mapping; one run of resting state (360 s); two runs of the monetary incentive delay task (432 s each); two runs of the go/no-go task (262 s each); two runs of the evocative images task (392 s each).

The tasks were presented to participants in the same order in which they have been covered in this work, namely the two runs of the monetary incentive delay task, followed by the two runs of the go/no-go task, followed by the two runs of the evocative images task. This was so that performance of the monetary incentive delay task would not be adversely affected by a changed emotional state following the presentation of aversive images during the evocative images task.

For each cohort, at the first visit only, a block of structural imaging was performed at the end of the session involving: a high resolution structural scan for anatomical registration and radiological reporting; a proton density scan to provide a second contrast for radiological reporting; a diffusion tensor imaging sequence for analysis of white matter. The resting state and diffusion tensor data will not be described further here, and will be described elsewhere. Structural images were used in spatial registration, but analysis of structural differences is not described here.

Total in-scanner time was approximately 80 minutes at the first visit, and 60 minutes at all subsequent visits. At every visit, all tasks were practiced outside of the scanner immediately prior to the start of the imaging session.

Structural Acquisition

At London and Cambridge (Siemens), high-resolution T1-weighted volumes were acquired using a magnetization-prepared rapid gradient echo (MPRAGE) sequence (TR = 2300 ms, TE = 2.98 ms, TI = 900 ms, flip angle = 9°, field of view = 256 mm, image matrix = 240 x 256) with a resolution of 1 mm isotropic. For the volume, 160 abutting straight sagittal slices were collected in an interleaved right to left manner, resulting in whole head coverage. Parallel imaging using Generalized Autocalibrating Partially Parallel Acquisition (GRAPPA) with an acceleration factor of 2 was performed.

At Manchester (Philips), high-resolution T1-weighted volumes were also acquired using an MPRAGE sequence (TR = 6.8 ms, TE = 3.1 ms, TI = 900 ms, flip angle = 9°, field of view = 270 mm, image matrix = 256 x 256) with an in-plane resolution of 1.055 x 1.055 mm and a slice thickness of 1.200 mm. For the volume, 126 abutting straight sagittal slices were collected in an interleaved right to left manner, resulting in whole head coverage. Parallel imaging using Sensitivity Encoding (SENSE) with an S reduction of 1.8 was performed.

These T1-weighted volumes followed ADNI protocols (Jack et al., 2008) to minimise inter-centre differences.

Functional Acquisition

At London and Cambridge (Siemens), functional imaging was performed using a multi-echo gradient echo echoplanar imaging (EPI) sequence (TR = 2000 ms, TE = 13 & 31 ms, flip angle = 80°, field of view = 225 mm, image matrix = 64 x 64) with an in-plane resolution of 3.516 x 3.516 mm and a slice thickness of 3.000 mm. The phase encoding direction was anterior to posterior. Echo spacing was 0.52 ms.

For each volume, 36 abutting oblique axial slices were collected in an ascending manner at an angle of around 30° to the anterior (AC) and posterior commissure (PC) line. This results in slightly less than whole brain coverage, with the most superior 9 mm not being imaged in most participants.

To achieve the desired resolution and repetition time, parallel imaging using GRAPPA with an acceleration factor of 2 was performed. The first three volumes of each functional run were automatically discarded to allow for T1 saturation effects and are not included in any number of volumes reported here.

At Manchester (Philips) identical parameters were used for EPI acquisition, but with 34 slices being collected and with acceleration achieved using SENSE.

Data Processing

Structural and functional processing was carried out using Analysis of Functional NeuroImages (AFNI) (version AFNI_2011_12_21_1014), FreeSurfer (version freesurfer-x86_64-unknown-linux-gnu-stable5-20130513), Advanced Normalization Tools (ANTs) (version ANTs-1.9.v4-Linux), and FMRIB Software Library's (FSL) (version 5.0.6) FMRI Expert Analysis Tool (*FEAT*) (version 6.00). All were run on CentOS 6.5 (version centos-release-6-5.el6.centos.11.2.x86_64).

T1 images were first corrected for intensity non-uniformity (AFNI's *3dUniformize*) before having extracerebral tissues removed (as part of FreeSurfer's *recon-all* pipeline). The whole brain images were then non-linearly registered to the MNI ICBM152 non-linear 6th generation symmetric average brain stereotaxic registration model in a 2 mm isotropic voxel space (ANTs' *antsRegistration*).

EPIs were corrected for slice timing effects (AFNI's *3dTshift*) before each volume was registered (AFNI's *3dvolreg*) to the volume most similar, in the least squares sense, to all others (in-house code). For each task a summary of movement was recorded as the

speed of motion over the runs (i.e. the sum of framewise displacements (FD) over the time taken for the runs, measured in mm/s).

The residual extracerebral tissues were then removed using FSL's Brain Extraction Tool (BET). Linear registration to the T1 image was achieved through a Boundary Based Registration (BBR) approach (FSL's *epi_reg*) before combining transformations to bring the EPIs into the same standard stereotaxic space as the transformed T1 (ANTs' *antsApplyTransforms*). Finally, these were smoothed with a three-dimensional Gaussian kernel of full width at half maximum of 6.0 mm (i.e. standard deviation = 2.5 mm) (AFNI's *3dBlurInMask*).

fMRI Task Modelling

Task processing and modelling was carried out using E-Prime (version 2.0.8.90), Microsoft Office Excel 2007 (version 12.0.4518.1014), in-house Python (version 2.7.6) scripts, and FSL.

Data from task responses were processed into usable formats (E-Prime's *E-DataAid*) before behavioural data and timings were extracted (*Excel*) and processed further

(Python scripts) into 3-column-format text files for each event type for compatibility with *FEAT*.

FMRIB's Improved Linear Modelling (FILM) prewhitening was performed on all voxel time courses. Estimates of six motion parameters (translations in the three orthogonal directions along with pitch, roll and yaw) calculated during preprocessing (AFNI's *3dvolreg*) were included in each model as confounding explanatory variables.

In all models convolution with a haemodynamic response function (HRF) was performed, this being FSL's commonly used gamma function with standard deviation 3 s and mean lag 6 s. No temporal derivatives were used in any model. All models had the same temporal filtering applied to them as was done to the image data.

Monetary Incentive Delay Task

Nine explanatory variables were used for modelling the task itself. These were the three different general conditions – reward, neutral, or loss – with each of these having three potential phases – anticipation, successful outcome, or unsuccessful outcome. 'Anticipation' was modelled as a block beginning at the cue (an arrow or line) onset and ending at the trial (a star) onset (these blocks lasting between approximately 3 s and 5

s). 'Outcome' was modelled as an immediately abutting block beginning at the trial (a star) onset and ending two seconds later. A high-pass filter cutoff of periods above 50 s was applied to both the data and the model. The contrast further explored in this work is that of 'reward anticipation' compared with 'neutral anticipation', with 'reward anticipation' being expected to show greater BOLD response (Knutson et al., 2001).

Go/No-Go Task

Two explanatory variables were used for modelling the task itself, one for 'successful no-go' and the other for 'unsuccessful no-go'. These were modelled against an implicit baseline of 'go'. Both 'successful no-go' and 'unsuccessful no-go' were modelled as events lasting 0.1 s. A high-pass filter cutoff of periods above 120 s was applied to both the data and the model. The contrast further explored in this work is that of 'successful no-go' compared with the implicit baseline of 'go', with 'successful no-go' being expected to show greater BOLD response (Garavan et al., 2003: 2003).

Evocative Images Task

Two explanatory variables were used for modelling the task itself, one for 'aversive' images and the other for 'neutral' images. Both 'aversive' and 'neutral' were modelled

as blocks lasting 32.4 s. A high-pass filter cutoff of periods above 100 s was applied to both the data and the model. The contrast further explored in this work is that of 'aversive' compared with 'neutral' images, with 'aversive' images being expected to show greater BOLD response (Asensio et al., 2010).

Higher Level Analysis

FEAT was used to run all the models discussed above within a general linear model framework. As each task was run twice in each imaging session the mean of the results for both runs was used in all higher level analyses.

This voxelwise analysis was extended to a group level in a mixed-effects analysis using FSL's FLAME 1 (1-sample t-test) controlling for centre, age, and sex. In calculating the whole brain group maps as part of the task characterisation investigation, data from the baseline session of the 43 inter-centre participants were used (a between-centre factor was included in the model). The Z statistic images shown in this work for the evocative and go/no-go tasks were thresholded using clusters determined by $Z > 3.1$ (i.e. an initial uncorrected cluster forming threshold of $p < 0.001$) and a (corrected) cluster significance threshold of $p < 0.05$. These initial cluster thresholds are higher than those commonly seen, and follow the advice given by Woo et al. (2014) relating to minimum

valid thresholds. The equivalent images for the monetary incentive delay task were thresholded using clusters determined by $Z > 4.5$ and a (corrected) cluster significance threshold of $p < 0.05$. This initial cluster threshold was raised compared with the other tasks due to the relatively stronger response expected in comparison to the other tasks, so that clusters would still be able to form and be interpretable. This group analysis was performed on the whole brain, insofar as including all those voxels which all participants had in common (areas outside this common coverage are shown masked in figures).

For the tasks which have temporal characteristics similar to block designs (monetary incentive delay and evocation) the contrasts' mean percentage signal changes within their ROIs were calculated (FSL's *Featquery*), while for the fast event-related design (go/no-go) arbitrary units based on the parameter estimates were used as percentage signal change is not usefully interpretable in this case.

Inter-Centre Differences

Non-image statistical analysis was carried out using IBM SPSS Statistics (version 22.0). When appropriate, values are given as mean ± standard deviation.

Between centre differences were tested for using one-way analysis of variance (ANOVA). When significant differences were found between centres Tukey's honestly significant difference (HSD) was used as the post-hoc test. Heterogeneity of variance was examined using Levene's test, and if found to be significant ($p < 0.05$) Welch's F was used. Post-hoc testing for data not meeting the homogeneity of variance assumption was carried out using the Games Howell method. Normality of data from each centre was tested using the Shapiro-Wilk method, and, if found to be significantly ($p < 0.05$) skewed, a non-parametric Kruskal-Wallis test performed in place of an ANOVA. Post-hoc tests for data examined using a non-parametric approach were carried out using the Mann-Whitney U test. All reported p values are those before any correction for either the number of tasks, or the number of tests carried out on the behavioural and summary imaging measures of those tasks, but they have been corrected for the number of post-hoc tests carried out for a particular measure.

FEAT was used to perform a voxelwise ANOVA, examining between centre differences to produce F statistic images of the whole brain for each task.

Results

Participants

A summary of the groupings and participant information is given in Table 1. No differences were found between centres for age, sex, or handedness, consistent with the matching process.

Each of the three tasks - monetary incentive delay, go/no-go, and evecative images - will be fully covered in turn, with each broken down into its meta-analysis/ROI, task characterisation, and inter-cetre differences.

Monetary Incentive Delay - ALE Meta-Analysis

For the monetary incentive delay task, we identified an initial total of 487 studies from searches on PubMed, and 170 from the BrainMap database, with 156 of the latter being duplicates of the former. This left a total of 501 studies. After abstract screening (501 studies) and full-text review (90 studies), 17 studies remained, representing 292 healthy participants with a total of 170 activation foci, shown in Table 2. Four clusters were found after carrying out the ALE analysis, the two largest of these being focused on the anterior region of the left and right putamen and overlapping with portions of caudate, nucleus accumbens, and globus pallidus (all bilaterally). All clusters found through ALE analysis are listed in Supplementary Table 1 and are shown in Figure 1. The ROI for this task was made up of bilateral 5 mm radius spheres centred at the co-ordinates ([L-R, P-A, I-S] in MNI space) [±14, 12, -4 mm], i.e. striatum (dorsal putamen/caudate).

Monetary Incentive Delay - Task Characterisation

Accuracy was not found to be different between the three types of trial (reward, neutral, and loss) ($F_{2,126} = 1.33$, $p = 0.27$), although response time was ($F_{2,126} = 4.31$, $p = 0.015$),

with response time of neutral trials being slower than loss trials (p = 0.003).
Supplementary Table 6 lists behavioural results.

The strongest observed response to reward anticipation (in terms of Z statistics) was in the primary visual cortex, with other strong responses in the caudate and anterior insula bilaterally. A spatially widespread response was observed in other visual areas and a large group of regions incorporating the striatum, thalamus, and insula, along with motor areas. No regions were seen to have a stronger response to neutral anticipation. Whole brain summary images of the reward anticipation > neutral anticipation contrast are shown in Figure 2, while more detailed images are shown in Supplementary Figure 1. Supplementary Table 3 lists the locations of clusters larger than 2 ml.

For this contrast, in the striatal ROI, the mean response (n = 43) was 0.53% ± 0.05 with a mean Z statistic of 5.84 ± 0.31. Supplementary Table 6 lists ROI results.

Monetary Incentive Delay - Inter-Centre Differences

In the monetary incentive delay task the accuracy of loss trials was different between the centres (Kruskal-Wallis, p = 0.006), with Manchester having lower accuracy than Cambridge (Mann-Whitney, p = 0.007). The response time of successful loss trials was

different between the centres (Kruskal-Wallis, p = 0.004), with Manchester being slower than Cambridge (Mann-Whitney, p = 0.012). Three of the other measures for the monetary incentive delay task – amount won, reward accuracy, and neutral accuracy – had skewed distributions (Shapiro-Wilk test) and so a non-parametric (Kruskal-Wallis) test was performed (p = 0.01, 0.04, and 0.03 respectively). These do not survive at the α = 0.05 level after a Bonferroni correction for the number of tests performed on the behavioural measures of this task (approximately seven independent tests), but are reported here for completeness. Appropriately corrected Mann-Whitney U post-hoc tests reveal that Manchester participants won less than those in London (p = 0.009), and had lower accuracy at reward trials than those in London (p = 0.021).

No imaging differences were found between centres at the whole brain (voxelwise) level. Unthresholded F maps are shown in Figure 5.

No differences were found between centres with regard to the ROI results.

Go/No-Go - ALE Meta-Analysis

For the go/no-go task, we identified an initial total of 353 studies from searches on PubMed, and 94 from the BrainMap database, with 80 of the latter being duplicates of the former. This left a total of 367 studies. After abstract screening (367 studies) and full-text review (189 studies), 12 studies remained, representing 243 healthy participants with a total of 180 activation foci, shown in Table 3. 12 clusters were found after carrying out the ALE analysis, distributed around the brain, but with a concentration around the striatum. All clusters found through ALE analysis are listed in Supplementary Table 2 and are shown in Figure 1. The ROI for this task was made up of bilateral 5 mm radius spheres centred at the co-ordinates [±22, 8, 6 mm], i.e. striatum (dorsal putamen).

Go/No-Go - Task Characterisation

Response time was found to be different between successful 'go' and unsuccessful 'no-go', with faster button presses for unsuccessful 'no-go' ($t = 6.69$, $p < 0.0001$, $df = 42$). Supplementary Table 7 lists behavioural results.

The strongest observed response to successful no-go (in terms of Z statistics) was in the anterior insula bilaterally, with other strong responses in right inferior frontal gyrus, putamen and thalamus. A spatially widespread response was observed across the brain, including right dorsolateral prefrontal cortex and bilateral motor areas. Only ventromedial prefrontal cortex was observed to have greater response to 'go' (implicit baseline). Whole brain summary images of the successful no-go > go (implicit baseline) contrast are shown in Figure 3, while more detailed images are shown in Supplementary Figure 2. Supplementary Table 4 lists the locations of clusters larger than 2 ml.

For this contrast, in the striatal ROI, the mean response (n = 43) was 0.36 arbitrary units ± 0.06 with a mean Z statistic of 6.27 ± 0.47. Supplementary Table 7 lists ROI results.

Go/No-Go - Inter-Centre Differences

No behavioural differences were found between centres for the go/no-go task.

No imaging differences were found between centres at the whole brain (voxelwise) level. Unthresholded F maps are shown in Figure 5.

No differences were found between centres with regard to the ROI results.

Evocative Images - Task Characterisation

Although the range of response times was large (280 to 1373 ms for neutral images and 267 to 1651 for aversive images) there was a very strong correlation between the two times (r = 0.94, p < 0.00001, df=58). The difference in response time (21 ms) was not significant between the aversive and neutral images (t = 1.86, p = 0.068, df = 42). Supplementary Table 8 lists behavioural results.

The strongest response observed to aversive images (in terms of Z statistics) was in visual cortex, with the strongest response outside of this region being in the amygdala bilaterally. Strong response was also observed in thalamus and medial hippocampus. Greater response to neutral images was observed in prefrontal and auditory cortices. Whole brain summary images of the aversive images > neutral images contrast are shown in Figure 4, while more detailed images are shown in Supplementary Figure 3. Supplementary Table 5 lists the locations of clusters larger than 2 ml.

For this contrast, in the amygdala ROI, the mean response (n = 43) was 0.32% ± 0.09 with a mean Z statistic of 3.90 ± 1.06. Supplementary Table 8 lists ROI results.

Rate of motion (i.e. mm/s) was not found to differ significantly for different tasks ($F_{2,126}$ = 2.61, p = 0.08).

Evocative Images - Inter-Centre Differences

No behavioural differences were found between centres for the evocative images task.

No imaging differences were found between centres at the whole brain (voxelwise) level. Unthresholded F maps are shown in Figure 5.

In the evocative images task, mean response (percentage signal change) within the amygdala ROI was found to differ between the centres ($F_{2,40} = 5.06$, $p = 0.01$), along with, as one would expect given the signal change, the mean Z statistic in this region ($F_{2,40} = 5.98$, $p = 0.005$). This was due to the Manchester participants having a lower response for this aversive images > neutral images contrast.

Discussion

We report here the establishment of an fMRI platform, ICCAM, to study mechanisms of relevance to relapse in addiction. Across three tasks investigating reward sensitivity, inhibitory control, and emotional reactivity, we have examined their characteristics, and inter-centre differences for behavioural, whole brain, and ROI measures. This study raised a number of issues, which we now discuss in turn.

Importantly our three tasks resulted in the expected pattern of brain responses consistent with existing evidence. Thus the monetary incentive delay task resulted in responses in regions such as the visual cortex, striatum, prefrontal and insula cortices consistent with previous studies (Knutson et al., 2001). The influence of variations in the task on the patterns of brain responses have been described elsewhere (Hommer et al., 2011; Limbrick-Oldfield et al., 2013). Though many people use the monetary incentive delay task, most adapt it to some extent so that it is no longer a standardised task. For instance, the ICCAM version of the monetary incentive delay task prioritized imaging 'anticipation of reward' since this primary contrast has been found altered in addiction and is of relevance to relapse. Therefore we were less interested in brain responses to loss or outcomes.

The pattern of brain response elicited by our monetary incentive delay task was consistent with that derived from the meta-analysis. Many fMRI studies of the monetary incentive delay task used spatially constrained approaches, i.e. analyses perform within ROIs of varying size, focused on striatal regions. Out of the 17 studies used here, 11 were not 'whole brain' analyses. Indeed, in the original fMRI monetary incentive delay study (Knutson et al., 2001), a limited acquisition of coronal slices was used, limiting coverage to a block including the striatum, and our own coverage is itself limited as can be seen throughout the figures (such as Figure 2). By comparison, of the 12 go/no-go studies included in the meta-analysis, none used such a spatially constrained approach.

The responses to the go/no-go task in inferior frontal gyrus, striatum, insula and thalamus were consistent with previous studies (Steele et al., 2013; Luijten et al., 2014). Our meta-analysis of similar go-nogo tasks resulted in a striatal ROI though this was more dorsal than the one derived from the meta-analysis of the monetary incentive delay task. This association between ventral striatum associated with reward processing and dorsal striatum with habit or compulsive behaviours, and the importance of fronto-corticostriatal loops in inhibitory control have been well documented (Everitt and Robbins, 2005; Koob and Volkow, 2010).

Although there is often a focus on the inferior frontal gyrus (IFG) when discussing go/no-go tasks, it did not emerge in our ALE meta-analysis (which closely follow the results presented in the task characterisation here). IFG response was observed in our task, though was weaker than insular or striatal responses. This might be explained by the 'simple' design task used here (and thus the strict criteria in our meta-analysis) while the majority of those in the literature used more complex designs (Criaud and Boulinguez, 2013). In the extensive ALE meta-analysis performed by Criaud and Boulinguez (2013) examining several facets of fMRI go/no-go tasks, it is also suggested that typical no-go activity is mostly driven by attention, not inhibition, though this is still a current topic of debate (Aron et al., 2014).

Both the go-nogo and monetary incentive delay task resulted in robust responses in the insula, particularly anterior insula. This brain region has been shown to be involved in self-regulation and reward seeking as well as in emotional awareness through integrating sensory information into cognitive, affective and physiological processes, along with being part of a task general network (Nelson et al., 2010; Menon and Uddin, 2010; Gu et al., 2013). With regard to addiction, the insula appears also to be involved with critical functions such as craving and the landmark description that damage to its structure substantially increased the likelihood of smoking cessation (Naqvi and Bechara, 2009; Garavan, 2010).

The evocative images task produced a robust response in the dorsal amygdala, along with inferior portions of the globus pallidus, with the highest response near the amygdala overlapping with the predetermined amygdala ROI. Such a pattern is consistent with previous studies using an evocative task or one that requires emotional processing (Costafreda et al., 2008; Sergerie et al., 2008). We were particularly interested in demonstrating a robust response in the amygdala since dysregulation in this region is implicated in relapse vulnerability in addiction, in particular those involving stress (Koob et al., 2014).

Even though this comparison between centres did not utilize a travelling participants design such as those of (Friedman et al., 2008; Suckling et al., 2012; Gee et al., 2015), it demonstrates that different groups of participants at different centres produce markedly similar responses to the tasks in our ICCAM platform. Recent explorations of both functional and structural neuroimages acquired from multiple centres have unequivocally demonstrated high levels of within- and between-centre reliability as well as small between-centre variances relative to the total variance (Suckling et al., 2012; Gee et al., 2015).

However, the lack of significant whole brain differences in the participants examined here does not necessarily imply that with larger groupings and different patient populations there would not be differences observed.

Although much effort was made to run the study in as similar a manner possible at each centre, there were inevitably slight differences between the experimental setups. From the voxelwise F statistic images in the Evocative Images task (Figure 5) a trend to a center difference was focused around the amygdala and was driven by the Manchester group. One factor may have been the means by which images were projected, which was almost identical in London and Cambridge but differed in Manchester where images were projected in a different manner, creating a less bright image and so possibly less salient, creating a smaller difference in activity between the aversive and neutral images.

Although in this analysis we have explored differences between centres, in the patient study itself participants were recruited so that there would be a roughly equal proportion of cases to controls at each centre, with centre also being included as a covariate in all analyses. Centre was also used as a covariate in the characterisation of the tasks.

Conclusion

We have demonstrated here the establishment of an fMRI platform involving three different tasks, repeated at multiple sessions and at three different centres. The establishment of this platform was critical to provide a framework to explore three key processes in the neurobiology of relapse vulnerability in addiction: reward; inhibitory control; and emotional regulation. This allows for an evidence base to inform future development in treatment to be provided within reasonable time periods. Future papers will present the results of these tasks in our healthy and patient groups, and under pharmacological modulation.

Acknowledgements

[*]ICCAM Platform collaborators

David Nutt, Anne Lingford-Hughes, Louise Paterson, John McGonigle, Remy Flechais, Csaba Orban, Bill Deakin, Rebecca Elliott, Anna Murphy, Eleanor Taylor, Trevor Robbins, Karen Ersche, John Suckling, Dana Smith, Laurence Reed, Filippo Passetti, Luca Faravelli, David Erritzoe, Inge Mick, Nicola Kalk, Adam Waldman, Liam Nestor, Shankar Kuchibatla, Venkataramana Boyapati, Antonio Metastasio, Yetunde Faluyi, Emilio Fernandez-Egea, Sanja Abbott, Barbara Sahakian, Valerie Voon, Ilan Rabiner

References

Aron AR, Robbins TW and Poldrack RA. (2014) Inhibition and the right inferior frontal cortex: one decade on. *Trends Cogn Sci* 18(4): 177-185.

Asensio S, Romero MJ, Palau C, et al. (2010) Altered neural response of the appetitive emotional system in cocaine addiction: an fMRI Study. *Addict Biol* 15(4): 504-516.

Bartra O, McGuire JT and Kable JW. (2013) The valuation system: a coordinate-based meta-analysis of BOLD fMRI experiments examining neural correlates of subjective value. *Neuroimage* 76: 412-427.

Berry SM, Connor JT and Lewis RJ. (2015) The platform trial: an efficient strategy for evaluating multiple treatments. *JAMA* 313(16): 1619-1620.

Bustamante JC, Barros-Loscertales A, Costumero V, et al. (2014) Abstinence duration modulates striatal functioning during monetary reward processing in cocaine patients. *Addict Biol* 19(5): 885-894.

Connolly CG, Foxe JJ, Nierenberg J, et al. (2012) The neurobiology of cognitive control in successful cocaine abstinence. *Drug Alcohol Depend* 121(1-2): 45-53.

Costafreda SG, Brammer MJ, David AS, et al. (2008) Predictors of amygdala activation during the processing of emotional stimuli: a meta-analysis of 385 PET and fMRI studies. *Brain Res Rev* 58(1): 57-70.

Criaud M and Boulinguez P. (2013) Have we been asking the right questions when assessing response inhibition in go/no-go tasks with fMRI? A meta-analysis and critical review. *Neurosci Biobehav Rev* 37(1): 11-23.

Eickhoff SB, Bzdok D, Laird AR, et al. (2012) Activation likelihood estimation meta-analysis revisited. *Neuroimage* 59(3): 2349-2361.

Eickhoff SB, Laird AR, Grefkes C, et al. (2009) Coordinate-based activation likelihood estimation meta-analysis of neuroimaging data: a random-effects approach based on empirical estimates of spatial uncertainty. *Hum Brain Mapp* 30(9): 2907-2926.

Everitt BJ and Robbins TW. (2005) Neural systems of reinforcement for drug addiction: from actions to habits to compulsion. *Nat Neurosci* 8(11): 1481-1489.

Filbey FM, Claus ED, Morgan M, et al. (2012) Dopaminergic genes modulate response inhibition in alcohol abusing adults. *Addict Biol* 17(6): 1046-1056.

Forman SD, Dougherty GG, Casey BJ, et al. (2004) Opiate addicts lack error-dependent activation of rostral anterior cingulate. *Biol Psychiatry* 55(5): 531-537.

Fox PT, Laird AR, Fox SP, et al. (2005) BrainMap taxonomy of experimental design: description and evaluation. *Hum Brain Mapp* 25(1): 185-198.

Friedman L, Stern H, Brown GG, et al. (2008) Test-retest and between-site reliability in a multicenter fMRI study. *Hum Brain Mapp* 29(8): 958-972.

Fusar-Poli P, Placentino A, Carletti F, et al. (2009) Functional atlas of emotional faces processing: a voxel-based meta-analysis of 105 functional magnetic resonance imaging studies. *J Psychiatry Neurosci* 34(6): 418-432.

Garavan H. (2010) Insula and drug cravings. *Brain Struct Funct* 214(5-6): 593-601.

Garavan H, Ross TJ, Kaufman J, et al. (2003) A midline dissociation between error-processing and response-conflict monitoring. *Neuroimage* 20(2): 1132-1139.

Garavan H, Ross TJ, Murphy K, et al. (2002) Dissociable executive functions in the dynamic control of behavior: Inhibition, error detection, and correction. *Neuroimage* 17(4): 1820-1829.

Gee DG, McEwen SC, Forsyth JK, et al. (2015) Reliability of an fMRI paradigm for emotional processing in a multisite longitudinal study. *Hum Brain Mapp*.

George DT, Gilman J, Hersh J, et al. (2008) Neurokinin 1 receptor antagonism as a possible therapy for alcoholism. *Science* 319(5869): 1536-1539.

Gilman JM and Hommer DW. (2008) Modulation of brain response to emotional images by alcohol cues in alcohol-dependent patients. *Addict Biol* 13(3-4): 423-434.

Gu X, Hof PR, Friston KJ, et al. (2013) Anterior insular cortex and emotional awareness. *J Comp Neurol* 521(15): 3371-3388.

Hasler G, Luckenbaugh DA, Snow J, et al. (2009) Reward processing after catecholamine depletion in unmedicated, remitted subjects with major depressive disorder. *Biol Psychiatry* 66(3): 201-205.

Hommer DW, Bjork JM and Gilman JM. (2011) Imaging brain response to reward in addictive disorders. *Ann N Y Acad Sci* 1216: 50-61.

Jack CR, Jr., Bernstein MA, Fox NC, et al. (2008) The Alzheimer's Disease Neuroimaging Initiative (ADNI): MRI methods. *J Magn Reson Imaging* 27(4): 685-691.

Jia Z, Worhunsky PD, Carroll KM, et al. (2011) An initial study of neural responses to monetary incentives as related to treatment outcome in cocaine dependence. *Biol Psychiatry* 70(6): 553-560.

Kaufman JN, Ross TJ, Stein EA, et al. (2003) Cingulate hypoactivity in cocaine users during a GO-NOGO task as revealed by event-related functional magnetic resonance imaging. *J Neurosci* 23(21): 7839-7843.

Keuken MC, Muller-Axt C, Langner R, et al. (2014) Brain networks of perceptual decision-making: an fMRI ALE meta-analysis. *Front Hum Neurosci* 8: 445.

Knutson B, Adams CM, Fong GW, et al. (2001) Anticipation of increasing monetary reward selectively recruits nucleus accumbens. *J Neurosci* 21(16): RC159.

Knutson B, Bjork JM, Fong GW, et al. (2004) Amphetamine modulates human incentive processing. *Neuron* 43(2): 261-269.

Koob G and Kreek MJ. (2007) Stress, dysregulation of drug reward pathways, and the transition to drug dependence. *Am J Psychiatry* 164(8): 1149-1159.

Koob GF, Buck CL, Cohen A, et al. (2014) Addiction as a stress surfeit disorder. *Neuropharmacology* 76 Pt B: 370-382.

Koob GF and Volkow ND. (2010) Neurocircuitry of addiction. *Neuropsychopharmacology* 35(1): 217-238.

Li CS and Sinha R. (2008) Inhibitory control and emotional stress regulation: neuroimaging evidence for frontal-limbic dysfunction in psycho-stimulant addiction. *Neurosci Biobehav Rev* 32(3): 581-597.

Limbrick-Oldfield EH, van Holst RJ and Clark L. (2013) Fronto-striatal dysregulation in drug addiction and pathological gambling: Consistent inconsistencies? *Neuroimage Clin* 2: 385-393.

Lingford-Hughes AR, Welch S, Peters L, et al. (2012) BAP updated guidelines: evidence-based guidelines for the pharmacological management of substance abuse, harmful use, addiction and comorbidity: recommendations from BAP. *J Psychopharmacol* 26(7): 899-952.

Loree AM, Lundahl LH and Ledgerwood DM. (2014) Impulsivity as a predictor of treatment outcome in substance use disorders: Review and synthesis. *Drug Alcohol Rev*.

Luijten M, Machielsen MW, Veltman DJ, et al. (2014) Systematic review of ERP and fMRI studies investigating inhibitory control and error processing in people with substance dependence and behavioural addictions. *J Psychiatry Neurosci* 39(3): 149-169.

Menon V and Uddin LQ. (2010) Saliency, switching, attention and control: a network model of insula function. *Brain Struct Funct* 214(5-6): 655-667.

Naqvi NH and Bechara A. (2009) The hidden island of addiction: the insula. *Trends Neurosci* 32(1): 56-67.

Nelson SM, Dosenbach NU, Cohen AL, et al. (2010) Role of the anterior insula in task-level control and focal attention. *Brain Struct Funct* 214(5-6): 669-680.

Noel X, Brevers D and Bechara A. (2013) A neurocognitive approach to understanding the neurobiology of addiction. *Curr Opin Neurobiol* 23(4): 632-638.

Paterson LM, Flechais RS, Murphy A, et al. (2015) The Imperial College Cambridge Manchester (ICCAM) platform study: An experimental medicine platform for evaluating new drugs for relapse prevention in addiction. Part A: Study description. *J Psychopharmacol* 29(9): 943-960.

Phan KL, Wager T, Taylor SF, et al. (2002) Functional neuroanatomy of emotion: a meta-analysis of emotion activation studies in PET and fMRI. *Neuroimage* 16(2): 331-348.

Schlagenhauf F, Juckel G, Koslowski M, et al. (2008) Reward system activation in schizophrenic patients switched from typical neuroleptics to olanzapine. *Psychopharmacology (Berl)* 196(4): 673-684.

Schouw ML, De Ruiter MB, Kaag AM, et al. (2013) Dopaminergic dysfunction in abstinent dexamphetamine users: results from a pharmacological fMRI study using a reward anticipation task and a methylphenidate challenge. *Drug Alcohol Depend* 130(1-3): 52-60.

Sergerie K, Chochol C and Armony JL. (2008) The role of the amygdala in emotional processing: a quantitative meta-analysis of functional neuroimaging studies. *Neurosci Biobehav Rev* 32(4): 811-830.

Simmonds DJ, Pekar JJ and Mostofsky SH. (2008) Meta-analysis of Go/No-go tasks demonstrating that fMRI activation associated with response inhibition is task-dependent. *Neuropsychologia* 46(1): 224-232.

Sinha R and Li CS. (2007) Imaging stress- and cue-induced drug and alcohol craving: association with relapse and clinical implications. *Drug Alcohol Rev* 26(1): 25-31.

Steele VR, Aharoni E, Munro GE, et al. (2013) A large scale (N=102) functional neuroimaging study of response inhibition in a Go/NoGo task. *Behav Brain Res* 256: 529-536.

Suckling J, Barnes A, Job D, et al. (2012) The Neuro/PsyGRID calibration experiment: identifying sources of variance and bias in multicenter MRI studies. *Hum Brain Mapp* 33(2): 373-386.

Turkeltaub PE, Eden GF, Jones KM, et al. (2002) Meta-analysis of the functional neuroanatomy of single-word reading: method and validation. *Neuroimage* 16(3 Pt 1): 765-780.

Turkeltaub PE, Eickhoff SB, Laird AR, et al. (2012) Minimizing within-experiment and within-group effects in Activation Likelihood Estimation meta-analyses. *Hum Brain Mapp* 33(1): 1-13.

Whiteford HA, Degenhardt L, Rehm J, et al. (2013) Global burden of disease attributable to mental and substance use disorders: findings from the Global Burden of Disease Study 2010. *Lancet* 382(9904): 1575-1586.

Woo CW, Krishnan A and Wager TD. (2014) Cluster-extent based thresholding in fMRI analyses: pitfalls and recommendations. *Neuroimage* 91: 412-419.

Wrase J, Schlagenhauf F, Kienast T, et al. (2007) Dysfunction of reward processing correlates with alcohol craving in detoxified alcoholics. *Neuroimage* 35(2): 787-794.

TABLE 1.

Participant information					
	London (n=15)	Cambridge (n=15)	Manchester (n=13)	ANOVA / Chi-square (n=15,15,13)	Combined (n=43)
Age (years)	40.5 ± 8.5 (21-53)	37.9 ± 9.3 (22-52)	41.0 ± 9.3 (25-56)	$F_{2,40} = 0.50$, $p = 0.61$	39.7 ± 8.9 (21-56)
# female	3	3	3	$X^2(2, N = 43) = 0.05$, $p = 0.97$	9
# left handed /ambidextrous	4/1	4/1	0/2	$X^2(4, N = 43) = 4.61$, $p = 0.33$	8/4

TABLE 2.

Studies included in the Monetary Incentive Delay ALE meta-analysis

Year	Author	Participants	Foci	Design	Scanner strength (T)	Whole brain analysis
2003	Knutson B et al.	12	10	Knutson	1.5	No
2004	Knutson B et al.	8	8	Knutson	3	Yes
2006	Juckel G et al.	10	9	Knutson	1.5	No
2007	Wrase J et al.	14	18	Knutson	1.5	No
2007	Wrase J et al.	16	2	Knutson	1.5	No
2008	Knutson B et al.	12	8	Knutson	1.5	Yes
2008	Schlagenhauf F et al.	10	12	Knutson	1.5	No
2008	Schmack K et al.	44	2	Knutson	1.5	No
2008	Strohle A et al.	10	7	Knutson	1.5	No
2009	Beck A et al.	19	6	Knutson	1.5	No
2010	Bjork JM et al.	24	10	Bjork	3	No
2011	de Greck M et al.	20	12	Knutson	1.5	Yes
2012	Balodis IM et al.	14	7	Knutson	3	No
2012	Cho YT et al.	30	18	Knutson	3	Yes
2012	Enzi B et al.	19	15	Knutson	1.5	Yes
2013	Edel MA et al.	12	4	Knutson	1.5	No
2013	Saji K et al.	18	22	Knutson	1.5	Yes
	Total	*292*	*170*			

TABLE 3.

Studies included in the Go/no-go ALE meta-analysis

Year	Author	Participants	Foci	Design	Scanner strength (T)	Whole brain analysis
2002	Garavan H et al.	14	16	X/Y Alternating	1.5	Yes
2003	Garavan H et al.	16	7	X/Y Alternating	1.5	Yes
2004	Hester R et al.	15	21	X/Y Alternating	1.5	Yes
2004	Kelly AM et al.	15	23	X/Y Alternating	1.5	Yes
2005	Maltby N et al.	11	5	X is Go, K is Nogo	1.5	Yes
2007	Epstein JN et al.	9	15	Multiple Go Cues, X is Nogo	1.5	Yes
2009	Welander-Vatn AS et al.	28	12	Multiple Go Cues, V is Nogo	1.5	Yes
2012	Bannbers E et al.	14	2	X/Y Alternating	3	Yes
2012	Sebastian A et al.	24	19	Multiple Go Cues, X is Nogo	3	Yes
2013	Sebastian A et al.	49	26	Multiple Go Cues, X is Nogo	3	Yes
2013	Sebastian A et al.	24	25	Multiple Go Cues, X is Nogo	3	Yes
2013	van der Salm SMA et al.	24	9	X/Y Alternating	3	Yes
	Total	*243*	*180*			

FIGURE 1.
Clusters found through the Activation Likelihood Estimation (ALE) meta-analyses. ALE was performed for each task with a False discovery rate (FDR) of p < 0.05 (corrected) and a minimum cluster volume of 0.6 ml.
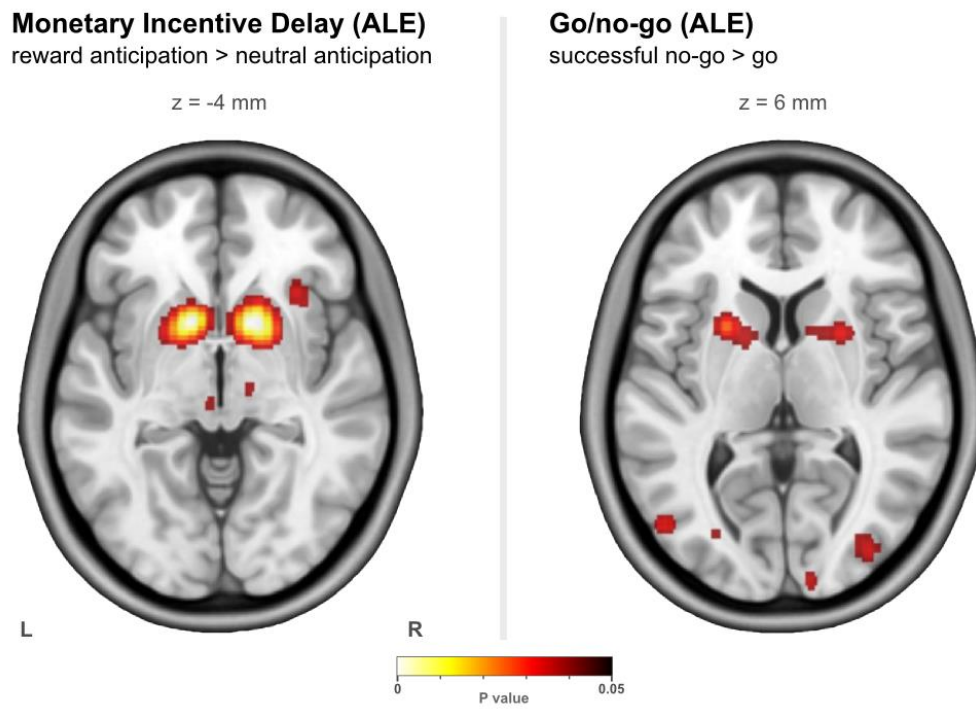
FIGURE 2.

The contrast of reward anticipation with neutral anticipation in the monetary incentive delay task in the combined group (n = 43), controlling for centre, age, and sex. Images were thresholded using clusters determined by Z > 4.5 and a (corrected) cluster significance threshold of p < 0.05. The slices shown were chosen such that all three intersect with the left side of the ROI used later in this work. The greyed out portion shows areas outside common coverage.
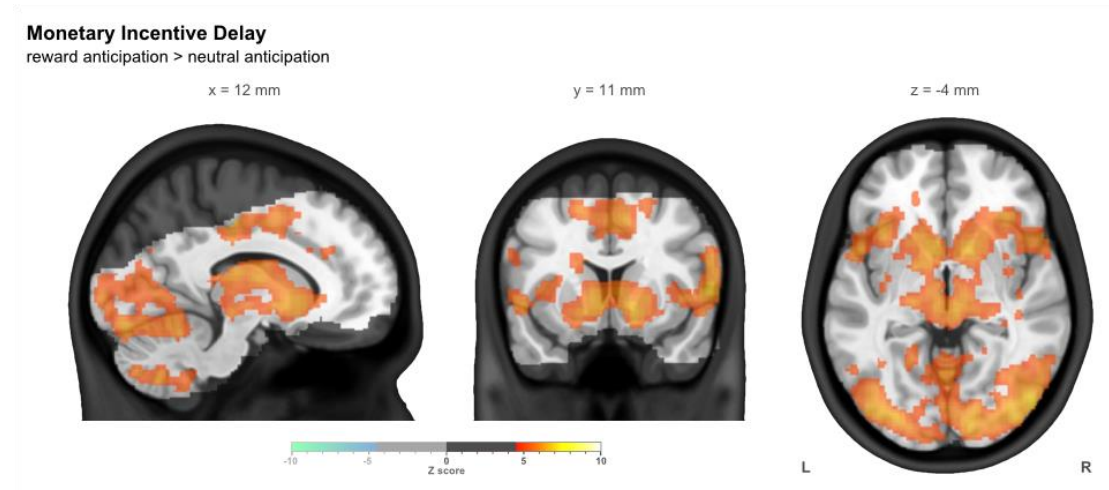
FIGURE 3.

The contrast of successful no-go with go (implicit baseline) in the go/no-go task in the combined group (n = 43), controlling for centre, age, and sex. Images were thresholded using clusters determined by Z > 3.1 and a (corrected) cluster significance threshold of p < 0.05. The slices shown were chosen such that all three intersect with the left side of the ROI used later in this work. The greyed out portion shows areas outside common coverage.
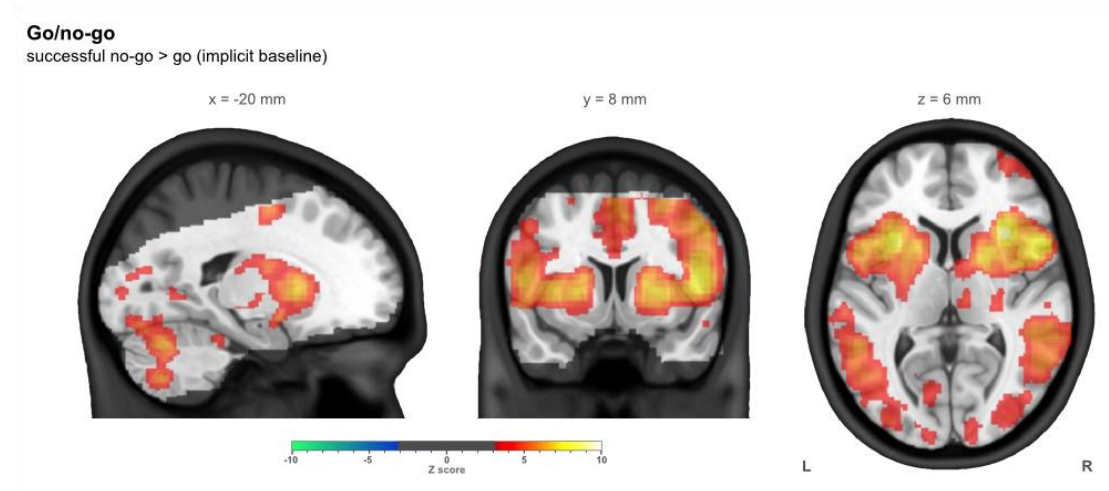
FIGURE 4.

The contrast of aversive images with neutral images in the evocative images task in the combined group (n = 43), controlling for centre, age, and sex. Images were thresholded using clusters determined by Z > 3.1 and a (corrected) cluster significance threshold of p < 0.05. The slices shown were chosen such that all three intersect with the left side of the ROI used later in this work. The greyed out portion shows areas outside common coverage.
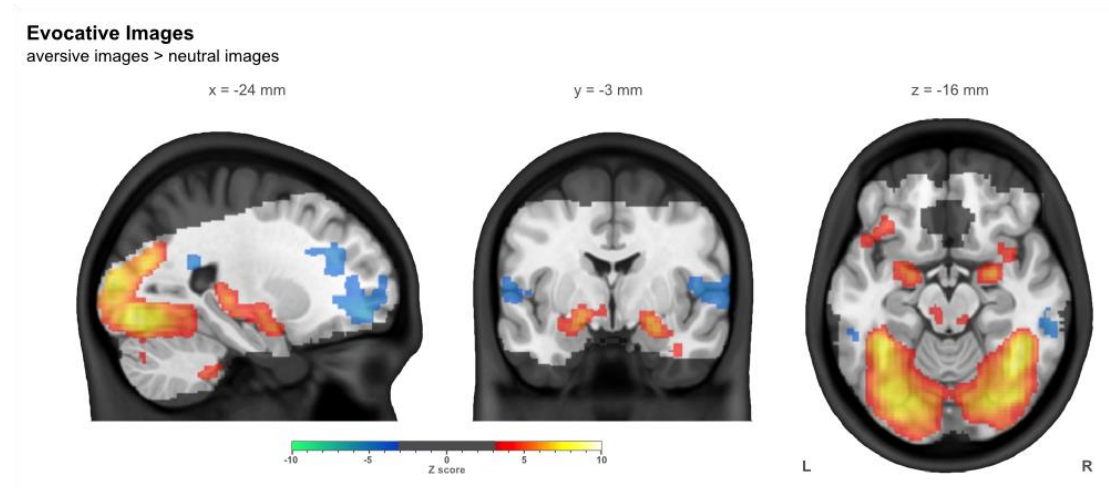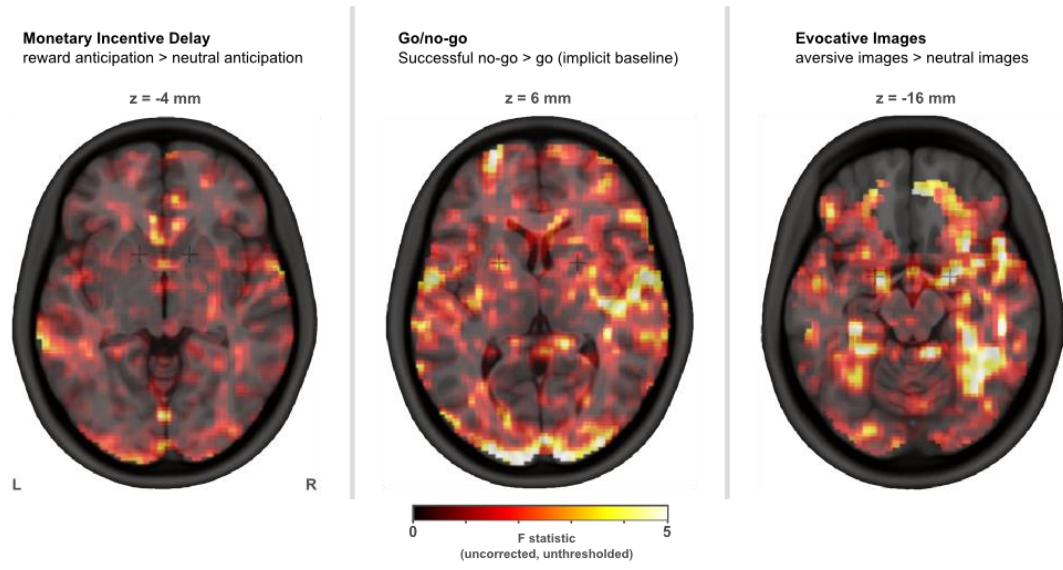

Evocative Images
aversive images > neutral images

FIGURE 5.
Unthresholded F maps exploring inter-centre differences. No significant imaging differences were found between centres at this whole brain (voxelwise) level.

SUPPLEMENTARY MATERIALS

SUPPLEMENTARY TABLE 1.

Monetary incentive delay: reward anticipation > neutral anticipation
17 experiments, 296 subjects

Region	Cluster volume (ml)	Weighted centre MNI coordinates (mm)		
		x	y	z
Right Putamen	7.60	15	9	-4
Left Putamen	6.91	-15	9	-6
Right Anterior Insula	0.94	33	23	-4
Left Inferior Frontal Precentral Gyrus	0.94	-50	9	28

Clusters are named according to the structure with the highest probability at that position in the Harvard-Oxford Cortical and Subcortical Structural Atlases.
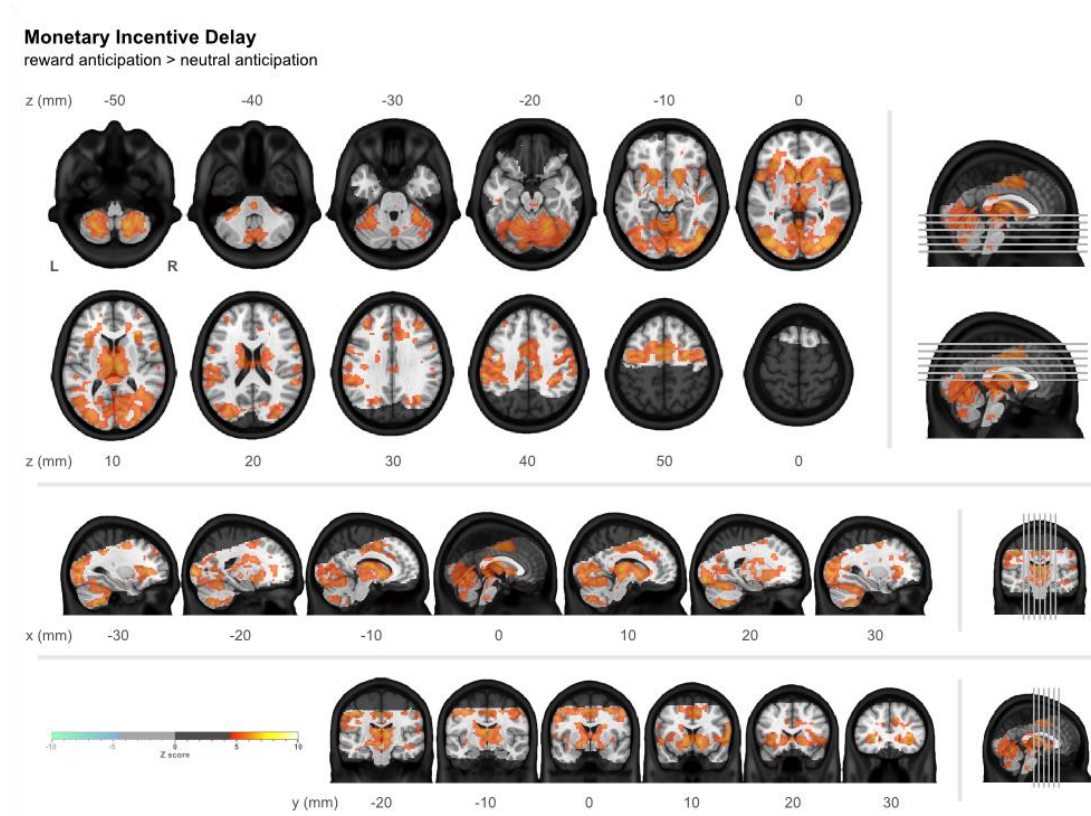
SUPPLEMENTARY TABLE 2.

Go/no-go: successful no-go > go
12 experiments, 246 subjects

Region	Cluster volume (ml)	Weighted centre MNI coordinates (mm)		
		x	y	z
Right Frontal Pole	2.77	35	40	24
Left Putamen	2.20	-20	7	4
Right Supplementary Motor Area	1.73	1	-1	63
Supramarginal Gyrus	1.49	49	-38	44
Superior Temporal Gyrus	1.34	56	-27	-2
Right Occipital Pole	1.33	30	-90	9
Precentral Gyrus	1.22	-45	-4	50
Right Lateral Occipital Cortex	1.20	31	-62	52
Right Putamen	0.82	21	6	6
Left Lateral Occipital Cortex	0.74	-50	-75	3
Right Lateral Occipital Cortex	0.70	48	-72	-2
Left Lateral Occipital Cortex	0.66	-22	-63	54

Clusters are named according to the structure with the highest probability at that position in the Harvard-Oxford Cortical and Subcortical Structural Atlases.

SUPPLEMENTARY FIGURE 1.

A detailed view of the contrast shown in Figure 2. The contrast of reward anticipation with neutral anticipation in the monetary incentive delay task in the combined group (n = 43), controlling for centre, age, and sex. Images were thresholded using clusters determined by Z > 4.5 and a (corrected) cluster significance threshold of p < 0.05. The greyed out portion shows areas outside common coverage.
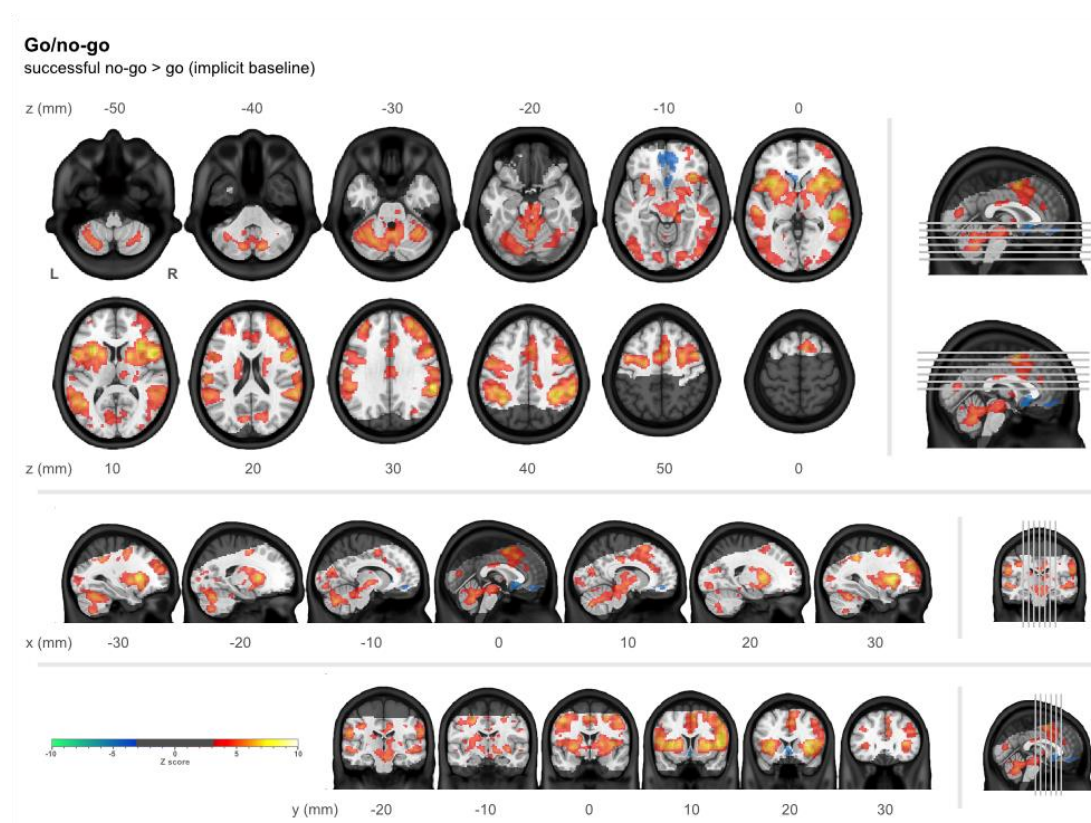
SUPPLEMENTARY TABLE 3.

Monetary incentive delay: reward anticipation > neutral anticipation

Region	Cluster volume (ml)	p	Local maxima Z score	MNI coordinates of maxima (mm)		
				x	y	z
Cluster 1 (Occipital Lobe)	185	< 0.0001				
Lateral Occipital Cortex, inferior division			7.05	48	-78	-6
Lingual Gyrus			6.97	-48	-66	4
Occipital Pole			6.94	-18	-98	2
Occipital Fusiform Gyrus			6.92	18	-90	-10
Occipital Pole			6.57	18	-94	-14
Cerebellum			6.55	18	-58	-52
Cluster 2 (Frontal Lobe)	175	< 0.0001				
Inferior Frontal Gyrus, pars opercularis			6.92	58	12	6
Frontal Operculum Cortex			6.92	32	30	8
Frontal Orbital Cortex			6.60	30	32	2
Supramarginal Gyrus, anterior division			6.60	56	-32	36
Cingulate Gyrus, anterior division			6.59	-28	30	4
Thalamus			6.58	8	-14	16
Cluster 3 (Frontal Lobe)	2.76	< 0.0001				
Paracingulate Gyrus			5.87	-34	40	34
Superior Frontal Gyrus			5.14	-32	38	44
Paracingulate Gyrus			4.83	-34	50	18
Cluster 4 (Parietal Lobe)	2.08	< 0.0001				
Postcentral Gyrus			5.68	32	-38	42
Postcentral Gyrus			5.66	38	-38	42
Postcentral Gyrus			4.84	42	-26	38

Coordinates (in MNI space) and Z score maxima for cluster-based statistical contrasts (all $Z > 4.5$, $p < 0.05$). Only clusters larger than 2 ml are shown. Clusters are first named by their general position according to the Talairach Daemon, while maxima are named according to the structure with the highest probability at that position in the Harvard-Oxford Cortical and Subcortical Structural Atlases.

SUPPLEMENTARY FIGURE 2.

A detailed view of the contrast shown in Figure 3. The contrast of successful no-go with go (implicit baseline) in the go/no-go task in the combined group (n = 43), controlling for centre, age, and sex. Images were thresholded using clusters determined by Z > 3.1 and a (corrected) cluster significance threshold of p < 0.05. The greyed out portion shows areas outside common coverage.
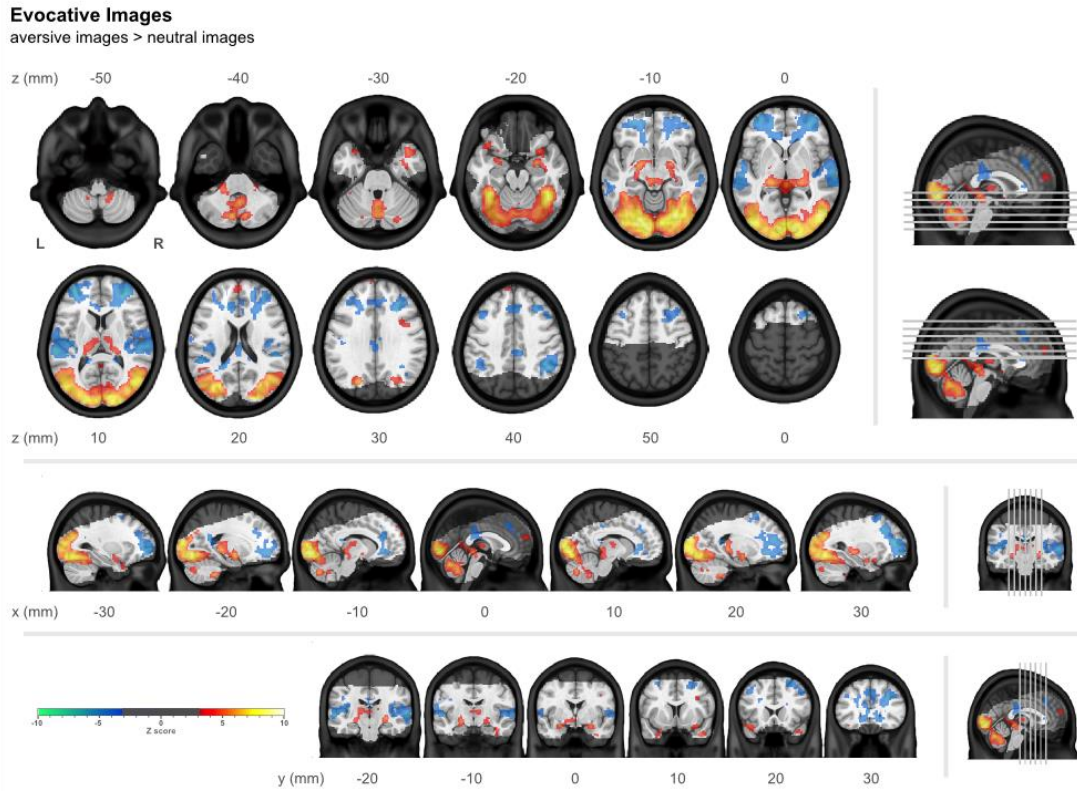
SUPPLEMENTARY TABLE 4.

Go/no-go: successful no-go > go (implicit baseline)

Region	Cluster volume (ml)	p	Local maxima Z score	MNI coordinates of maxima (mm)		
				x	y	z
Cluster 1 (Sub-lobar)	371	< 0.0001				
Insular Cortex			9.34	32	18	6
Subcallosal Cortex			8.38	-32	14	8
Supramarginal Gyrus, posterior division			8.34	60	-44	26
Superior Temporal Gyrus, posterior division			8.23	48	-28	-2
Inferior Frontal Gyrus, pars opercularis			8.02	48	8	10
Precentral Gyrus			7.81	50	8	6
Cluster 2 (Frontal Lobe)	9.2	< 0.0001				
Paracingulate Gyrus			5.97	-34	46	28
Paracingulate Gyrus			5.36	-30	54	20
Frontal Pole			5.20	-38	56	14
Paracingulate Gyrus			4.54	-36	46	16
Cluster 3 (Limbic Lobe)	3.096	0.0001				
Frontal Medial Cortex			-4.48	-10	50	-12
Frontal Medial Cortex			-4.42	12	46	-10
Frontal Medial Cortex			-4.21	4	48	-14
Paracingulate Gyrus			-4.14	6	36	-12
Frontal Medial Cortex			-3.99	-2	54	-8
Subcallosal Cortex			-3.40	-8	30	-8

Coordinates (in MNI space) and Z score maxima for cluster-based statistical contrasts (all $Z > 3.1$, $p < 0.05$). Only clusters larger than 2 ml are shown. Clusters are first named by their general position according to the Talairach Daemon, while maxima are named according to the structure with the highest probability at that position in the Harvard-Oxford Cortical and Subcortical Structural Atlases.

SUPPLEMENTARY FIGURE 3.

A detailed view of the contrast shown in Figure 4. The contrast of aversive images with neutral images in the evocative images task in the combined group (n = 43), controlling for centre, age, and sex. Images were thresholded using clusters determined by Z > 3.1 and a (corrected) cluster significance threshold of p < 0.05. The greyed out portion shows areas outside common coverage.

Evocative images: aversive images > neutral images

Region	Cluster volume (ml)	p	Local maxima Z score	MNI coordinates of maxima (mm)		
				x	y	z
Cluster 1 (Occipital Lobe)	182	< 0.0001				
Lateral Occipital Cortex, inferior division			8.83	48	-74	-2
Occipital Fusiform Gyrus			8.81	30	-78	-12
Lateral Occipital Cortex, inferior division			8.81	52	-70	6
Occipital Pole			8.74	18	-94	18
Lingual Gyrus			8.72	-20	-84	-10
Occipital Pole			8.69	-4	-92	-6
Cluster 2 (Frontal Lobe)	69.8	< 0.0001				
Frontal Pole			-6.71	34	50	10
Paracingulate Gyrus			-6.13	-34	54	8
Frontal Medial Cortex			-5.73	-26	52	-8
Middle Frontal Gyrus			-5.67	30	28	32
Paracingulate Gyrus,			-5.60	-32	46	8
Left Cerebral White Matter			-5.54	22	40	-4
Cluster 3 (Sub-lobar)	28.5	< 0.0001				
Amygdala			6.36	-20	-6	-12
Thalamus			6.22	-20	-30	0
Brain-Stem			6.17	-6	-30	-6
Amygdala			6.01	24	-4	-14
Thalamus			5.77	22	-30	0
Brain-Stem			5.65	4	-32	-2
Cluster 4 (Temporal Lobe)	19.8	< 0.0001				
Planum Temporale			-5.74	62	-22	6
Planum Temporale			-5.67	52	-30	12
Superior Temporal Gyrus, posterior division			-5.66	64	-22	2
Parietal Operculum Cortex			-5.48	50	-32	18
Superior Temporal Gyrus, anterior division			-5.41	64	-8	-2
Superior Temporal Gyrus, posterior division			-5.16	66	-30	4
Cluster 5 (Sub-lobar)	19.1	< 0.0001				
Cerebral White Matter			-6.51	-60	-30	10
Cingulate Gyrus, posterior division			-6.14	-50	-40	16
Thalamus			-5.28	-44	-20	10
Thalamus			-4.88	-56	-12	2
Cerebral White Matter			-4.76	-44	-24	16
Cerebral White Matter			-4.54	-64	-10	14
Cluster 6 (Parietal Lobe)	5.44	< 0.0001				
Supramarginal Gyrus, posterior division			-5.84	42	-46	40
Supramarginal Gyrus, posterior division,			-5.39	50	-50	42
Angular Gyrus			-5.14	38	-52	32
Lateral Occipital Cortex, superior division			-4.48	40	-64	34
Cluster 7 (Limbic Lobe)	3.94	< 0.0001				
Cingulate Gyrus, posterior division			-4.27	6	-30	38
Lateral Ventrical			-4.08	14	-38	16
Cerebral White Matter			-4.04	2	-22	20
Cerebral White Matter			-3.98	18	-42	12
Cingulate Gyrus, anterior division			-3.73	4	-14	28
Cingulate Gyrus, posterior division			-3.66	0	-28	30

Coordinates (in MNI space) and Z score maxima for cluster-based statistical contrasts (all Z > 3.1, p < 0.05). Only clusters larger than 2 ml are shown. Clusters are first named by their general position

according to the Talairach Daemon, while maxima are named according to the structure with the highest probability at that position in the Harvard-Oxford Cortical and Subcortical Structural Atlases.

SUPPLEMENTARY TABLE 6.

Monetary incentive delay: task characterisation and between centre examination				
	London (n=15)	Cambridge (n=15)	Manchester (n=13)	ANOVA (n=15,15,13)	Combined (n=43)
Amount won (£)	9.73 ± 3.26	10.37 ± 3.18	8.12 ± 1.33	$F_{2,40} = 2.38, p = 0.11$ [#]	9.47 ± 2.88
Accuracy: reward (%)	66 ± 12	68 ± 11	62 ± 6	$F_{2,40} = 1.45, p = 0.25$ [#]	66 ± 10
Accuracy: neutral (%)	63 ± 11	67 ± 11	58 ± 7	$F_{2,40} = 2.90, p = 0.07$ [#]	63 ± 11
Accuracy: loss (%)	64 ± 20	70 ± 21	50 ± 8	*Welch's* $F_{2,23.3} = 8.00, p = 0.002$ [‡]	62 ± 19
Hit response time: reward (ms)	211 ± 21	205 ± 25	224 ± 14	$F_{2,40} = 2.97, p = 0.06$	213 ± 22
Hit Response time: neutral (ms)	215 ± 22	209 ± 24	226 ± 9	$F_{2,40} = 2.49, p = 0.10$	216 ± 21
Hit Response time: loss (ms)	207 ± 19	198 ± 22	219 ± 8	$F_{2,40} = 4.45, p = 0.018$ [‡]	208 ± 19
Striatal ROI: win anticipation > neutral anticipation (% signal) [a]	0.28 ± 0.28	0.30 ± 0.27	0.28 ± 0.30	$F_{2,40} = 0.02, p = 0.98$	0.28 ± 0.27
Striatal ROI: win anticipation > neutral anticipation (Z score) [a]	1.91 ± 2.05	2.35 ± 2.13	1.97 ± 2.04	$F_{2,40} = 0.19, p = 0.83$	2.08 ± 2.04
Motion (mm/s)	0.12 ± 0.21	0.07 ± 0.01	0.07 ± 0.02	$F_{2,40} = 0.90, p = 0.41$ [†]	0.09 ± 0.13

[†]Normality assumptions of at least one subgroup violated (Shapiro-Wilk test), but no significant differences between groups found using a non-parametric test (Kruskal-Wallis).

[‡]Normality assumptions of at least one subgroup violated (Shapiro-Wilk test), significant differences between groups also found using a non-parametric test (Kruskal-Wallis).

[#]Normality assumptions of at least one subgroup violated (Shapiro-Wilk test), significant differences between groups also found using a non-parametric test (Kruskal-Wallis), but are not significant after a Bonferroni correction for number of independent tests performed on this task (~ 7).

[a]These values represent the means of the raw numbers extracted on an individual basis. Higher values are reported in the main text after the full mixed effects model has been carried out, and accounting for centre, age, and sex.

SUPPLEMENTARY TABLE 7.

Go/no-go: task characterisation and between centre examination				
	London (n=15)	Cambridge (n=15)	Manchester (n=13)	ANOVA (n=15,15,13)	Combined (n=43)
Accuracy: go (%)	96 ± 6	94 ± 19	97 ± 5	$F_{2,40} = 0.53, p = 0.77$ [†]	96 ± 12
Accuracy: no-go (%)	65 ± 17	66 ± 16	71 ± 15	$F_{2,40} = 0.47, p = 0.63$	67 ± 16
Go response time (ms)	339 ± 75	313 ± 65	326 ± 57	$F_{2,40} = 0.55, p = 0.58$	326 ± 66
No-go response time (ms)	295 ± 79	278 ± 85	274 ± 48	$F_{2,40} = 0.33, p = 0.72$ [†]	283 ± 72
Striatal ROI: no-go > go (a.u.) [a]	0.22 ± 0.12	0.17 ± 0.14	0.26 ± 0.16	$F_{2,40} = 1.33, p = 0.28$	0.21 ± 0.14
Striatal ROI: no-go > go (Z score) [a]	1.46 ± 0.79	1.30 ± 0.99	1.41 ± 0.74	$F_{2,40} = 0.15, p = 0.87$	1.39 ± 0.83
Motion (mm/s)	0.06 ± 0.03	0.06 ± 0.02	0.05 ± 0.02	$F_{2,40} = 1.05, p = 0.36$ [†]	0.06 ± 0.02

[†]Normality assumptions of at least one subgroup violated (Shapiro-Wilk test), but no significant differences between groups found using a non-parametric test (Kruskal-Wallis).
[a]These values represent the means of the raw numbers extracted on an individual basis. Higher values are reported in the main text after the full mixed effects model has been carried out, and accounting for centre, age, and sex.

"No-go response time" is that of unsuccessful no-go. a.u. = arbitrary units.

SUPPLEMENTARY TABLE 8.

Evocative images: task characterisation and between centre examination					
	London (n=15)	Cambridge (n=15)	Manchester (n=13)	ANOVA (n=15,15,13)	Combined (n=43)
Neutral response time (ms)	750 ± 242	587 ± 172	680 ± 276	$F_{2,40} = 1.88, p = 0.17$ [†]	672 ± 236
Aversive response time (ms)	778 ± 255	596 ± 157	696 ± 289	$F_{2,40} = 2.20, p = 0.12$ [†]	689 ± 244
Difference in response time (aversive -neutral) (ms)	24 ± 119	9 ± 67	15 ± 82	*Welch's* $F_{2,25.2} = 0.14, p = 0.87$	17 ± 90
Amygdala ROI: aversive > neutral (% signal) [a]	0.31 ± 0.23	0.29 ± 0.26	0.02 ± 0.32	$F_{2,40} = 5.06, p = 0.01$ [‡]	0.21 ± 0.29
Amygdala ROI: aversive > neutral (Z score) [a]	1.54 ± 1.09	1.51 ± 1.13	0.26 ± 1.08	$F_{2,40} = 5.98, p = 0.005$	1.15 ± 1.23
Motion (mm/s)	0.09 ± 0.03	0.07 ± 0.03	0.08 ± 0.05	$F_{2,40} = 0.69, p = 0.51$ [†]	0.08 ± 0.04

[†]Normality assumptions of at least one subgroup violated (Shapiro-Wilk test), but no significant differences between groups found using a non-parametric test (Kruskal-Wallis).

[‡]Normality assumptions of at least one subgroup violated (Shapiro-Wilk test), significant differences between groups also found using a non-parametric test (Kruskal-Wallis).

[a]These values represent the means of the raw numbers extracted on an individual basis. Higher values are reported in the main text after the full mixed effects model has been carried out, and accounting for centre, age, and sex.